Ad Hoc Networks 47 (2016) 41–52

Contents lists available at ScienceDirect

Ad Hoc Networks

journal homepage: www.elsevier.com/locate/adhoc

Traffic-aware contact plan design for disruption-tolerant space sensor networks

Juan A. Fraire*, Pablo G. Madoery, Jorge M. Finochietto

Universidad Nacional de Córdoba-CONICET, Argentina

ARTICLE INFO

Article history:
Received 21 January 2016
Revised 20 April 2016
Accepted 21 April 2016
Available online 3 May 2016

Keywords:
Delay and disruption tolerant networks
Satellite networks
Contact plan design

ABSTRACT

Delay and disruption tolerant networks (DTNs) are becoming an appealing solution for extending Internet boundaries across challenged network environments. In particular, if node mobility can be predicted as in space sensor networks (SSNs), routing schemes can take advantage of the a-priori knowledge of a contact plan comprising forthcoming communication opportunities. However, the design of such a plan needs to consider available spacecraft resources whose utilization can be optimized by exploiting the expected data which is largely foreseeable in typical Earth observation missions. In this work, we propose Traffic-Aware Contact Plan (TACP): a novel contact plan design procedure based on a Mixed Integer Linear Programming (MILP) formulation which exploits SSNs predictable properties in favor of delivering efficient and implementable contact plans for spaceborne DTNs. Finally, we analyze a low orbit SSN case study where TACP outperforms existing mechanisms and proves to be of significant impact on enhancing the delivery of sensed data from future space networks.

1. Introduction

Today, optical and radar images of our planet are being acquired continuously from orbit as they allows for a better understanding and improved management of the Earth and its environment. Traditionally, a single Low Earth Orbit (LEO) satellite sensor gathers data from sites across the world, including places inaccessible to ground-based data acquisition, making Earth observation from space an effective means of providing coverage across both space and time. Indeed, an ad-hoc orbiting network of spatially distributed autonomous wireless sensors (Space Sensor Network or SSN [1]) are opening new possibilities for unprecedented applications by significantly extending system coverage in both dimensions.

However, SSNs requires novel communication strategies in order to efficiently manage and operate the system from Earth. In general, transmitting commands and retrieving telemetry and data from each SSN node individually requires several Earth to space links in order to access the entire system. Even though this approach might result reasonable for small-sized SSNs, a more efficient solution is devised by relying on inter-satellite links (ISLs) to cooperatively pass sensed data through the network to the final ground destination [2]. Nonetheless, in contrast with sensor networks on Earth, links between nodes might suffer from severe disruption due to orbital mechanics [3]. Since existing communication protocols assume a persistent connection between the origin of the data and its destination they either require significant adjustments [4], or demand strict flight-formation requirements [5], or directly fail to perform under this challenging conditions [6].

To embrace this type of disruptive communications, a research group led by Vinton Cerf had proposed to overcome the limitations of persistent end-to-end connectivity by implementing a store-carry-and-forward overlay network on top of existing networks [7,8]. This architecture was named Delay and Disruption Tolerant network (DTNs) [9] and is currently being maintained and discussed by the DTN Working Group of the Internet Engineering Task Force [10] and the Consultative Committee for Space Data Systems (CCSDS) [11]. Among the extensive research work on DTN, its architecture [12], the Bundle Protocol [13] and Contact Graph Routing (CGR) [14], are specifically designed to cope with networks in space and other extreme environments. Furthermore, these advances have been successfully flight-tested in the DINET deep-space mission [15] validating NASA's Interplanetary Overlay Network (ION) [16] implementation. Also, DTN supported the download of scientific data of the UK-DMC satellite from a Cisco router in LEO orbit [17]. As a result, DTN is becoming an appealing network paradigm to support not only future SSNs but also many other applications with relaxed round trip times requirements [18].

Since the mobility of SSN nodes is ruled by orbital mechanics, their future position and orientation can be accurately known

* Corresponding author.
E-mail address: juanfraire@unc.edu.ar, juanfraire@gmail.com (J.A. Fraire).

http://dx.doi.org/10.1016/j.adhoc.2016.04.007
1570-8705/

Table 1
Case study time lapses and orbital parameters.

Time interval start	January-1st, 2016, 00: 00: 00
Time interval end	January-1st, 2016, 03: 30: 00
Bstar coefficient (/ER)	0
Inclination (deg)	98°
RAAN (deg)	0°, 5°, 10°, and 15°
Eccentricity	0 (circular orbit)
Argument of perigee (deg)	180°, 185°, 190°, 195°
Mean anomaly (deg)	0°
Mean motion (rev/day)	14.9162 rev/day
Height (Km)	600 Km

in advance. Therefore, by combining this information with precise communication models, a *contact plan* comprising all forthcoming transmission opportunities (also known as *contacts*) in the SSN system can be obtained. Indeed, the provision of a contact plan to each of the orbiting nodes allows distributed routing schemes such as CGR to efficiently forward data towards its final destination [19]. Besides the contact plan, traffic also becomes predictable in SSNs as the generation and transmission of data acquisitions from space are typically managed and scheduled by a centralized Mission Operations and Control (MOC) center [20]. As a result, traffic information might be used to support the design and optimization of the contact plan improving the SSN data delivery time and resource usage.

In this work, we seek to investigate this performance improvement by integrating traffic information into a mixed integer linear programing (MILP) model named Traffic-Aware Contact Plan Design (TACP) that optimizes the contact plan for SSN systems. Along the paper, we characterize, analyze and evaluate the model and compare it with existing schemes to finally discuss the challenges and limitations of implementing TACP in an operative SSN system.

This work is organized as follows. In Section 2 we introduce the network model and the problem of contact plan optimization and design. Next, in Section 3 we present and describe TACP model parameters and formulation. Later, a case study is proposed and used as a performance benchmark in Section 4. Finally, we briefly discuss relevant concepts and TACP limitations in Section 5 to later draw conclusions and future work in Section 6.

2. System model

2.1. Contact topology model

In general, a *contact* stands for a forthcoming transmission opportunity and is defined by at least a start and end time and a source and destination node pair. To determine these parameters, communications subsystem attributes such as transmission power, modulation, bit-error-rate, among others can be combined with orbital dynamics [21] such as position, range, and attitude (orientation of the spacecraft and antenna in the inertial system) of each node. This procedure is essentially the same as those used in current single-spacecraft missions to predict space-to-earth contacts, but extended to embrace ISLs within the multiple nodes in the SSN. As a result, the set of all feasible contacts for all nodes in the system within a given *time interval* forms what we define a *contact topology*. This contact topology will need further refinement before becoming the final *contact plan* to be provisioned to the SSN system.

For example, consider a SSN of 4 satellites with the orbital parameters listed in Table 1, which are deliberately configured to have one node ahead of the other on the trajectory vector (by a 5° perigee argument) with a slight variation of the right ascension of the ascending node (RAAN) angle. This scenario is of particular interest for Earth observation missions as sensors on board the satellites are separated further apart with maximum distance (coverage) on populated areas while approaching each other in the poles [22]. In these areas, contacts become feasible between adjacent spacecrafts producing a train-like formation with a node separation of 500 Km where two directive point-to-point antennas (placed in front and back of each satellite) can optimize the link budget producing longer contacts. These communication opportunities can be exploited to transfer and aggregate data between orbiting nodes before its final download to a ground station.

By using SGP-4 [21] (a well-known satellite propagator), combined with a maximum communication range of 700 Km for ISL, we obtain the time evolving contact topology shown in Fig. 1. Although a single half-orbit of 56 min and 8 s is sufficient to illustrate the scenario as satellites orbit through the North-Pole, we consider a total time interval of 3 h and 30 min comprising 2 full orbits to be later proposed as the case study for TACP in Section 4.1. The resulting time evolving topology is captured by means of graphs, whose vertices and edges symbolize DTN nodes and their feasible contacts respectively. Specifically, the topology is discretized by a set of k time intervals $[t_k, t_{k+1}]$ or division points. Each state has a graph representing the communication opportunities within its interval duration ($i_k = t_k - t_{k-1} : 1 \leq k \leq K$). As a result, we encode the time evolution in two matrices $T = \{t_k\}$ and $I = \{i_k\}$ of size K, representing each k state starting time and interval duration respectively.

Regarding contact modeling, for every start and end of a contact, there is a k_a to k_{a+1} state evolution in the finite state machine. Indeed, a single contact can span multiple consecutive k states. Henceforth, an *arc* will represent the portion of a contact during a given k state. Also, each arc between node i and j at state k is parameterized by a capacity value (traffic volume) encoded in $c_{k,\,i,\,j}$. Particularly, 7 states and 9 arcs are sufficient to describe the first half orbit of the contact topology with 3 contacts between 4 orbiting sensors. It is worth noting that the state k_4 represents the train-like formation over the pole (N_1 to N_2, N_2 to N_3 and N_3 to N_4) with a duration of 1458 s. However, the linear formation is arranged and disarranged in incremental steps through states k_2, k_3, k_5 and k_6 providing useful transmission opportunities between the SSN.

2.2. Contact plan design

In general, SSN node resources are constrained due to weight, power, thermal and other physical limitations of spaceborne systems which can be translated to basic constraints of limited storage capacity and data rate. These constraints need to be taken into consideration at the planning stage in order to avoid memory exhaustion or congestion in the traffic flow of the SSN. Furthermore, interference generated to and from other space assets needs to be considered [23] as they might require the ban or reduction of contacts in the final contact plan [22].

Besides, the availability of communication resources such as antennas and transponders in the platform need to be specially considered in order to avoid scheduling conflicts once the contact plan is implemented in the final SSN. In particular, a node may have potential contacts with more than one node at a given time but be constrained to only make use of one of these opportunities due to these conflicting resources. Indeed, these constraints have previously been modeled and defined as *concurrent resources constraints* in [22] and are of particular importance as they usually involve solving a combinatorial problem before defining the final contact plan.

The simplest constraints are evidenced when a spacecraft antenna radiation pattern allows to reach two or more neighbors as shown in Fig. 2 (a). In this case, multiple access schemes could just automatically negotiate the channel usage; however, given the low

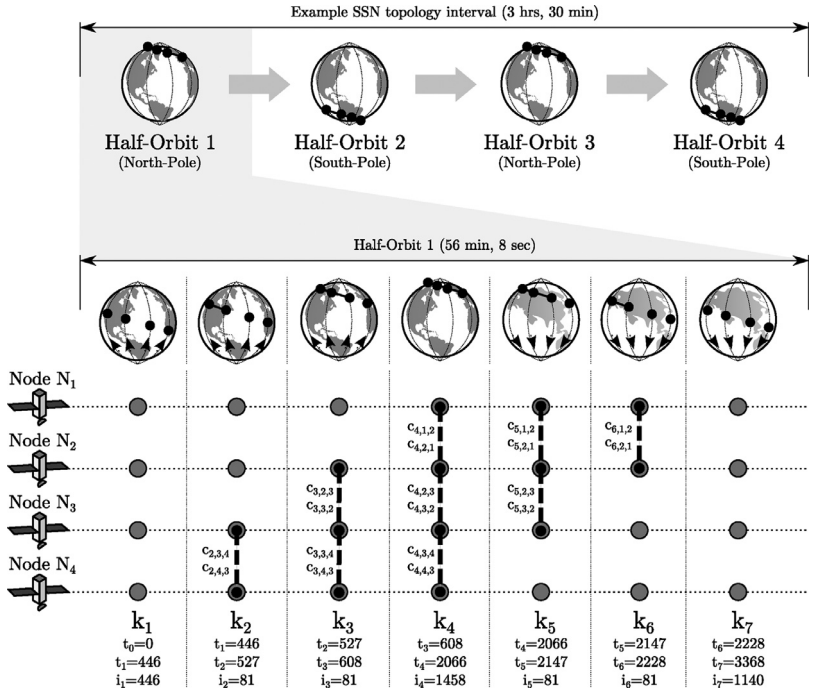

Fig. 1. Trajectory and contact topology model of the example SSN.

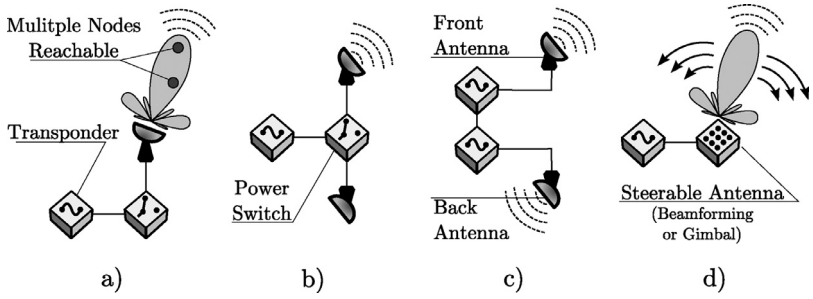

Fig. 2. Satellite architecture with (a) multiple target nodes, (b) a power switch, (c) two transponders, and (d) a steerable antenna.

probability of occurrence of this scenario in a highly sparse environment like space, and the overhead imposed by traditional negotiation procedures at ISL distances their implementation is discouraged for the general case [24]. Therefore, the more efficient usage of point-to-point links requires the system operator to decide which communication should be established in advance.

Furthermore, when a satellite platform is expected to accommodate ISL links from different directions, more than one antenna might need to be placed in the structure. For example, consider Fig. 2 (b), where a power switch allows to select the transmitter antenna. In this case, only one contact can be established at a given time even if more are feasible through each antenna in the contact topology. A more complex architecture is shown in Fig. 2 (c) where two simultaneous contacts can be implemented by two cooperative communications subsystems as long as the power supply can maintain both transponders active. However, if the power budget only allows for a single transponder to be enabled, the single contact limitation remains as in Fig. 2 (b). Finally, when considering electronically or mechanically steerable antenna techniques (i.e. beam-forming and gimbal-based antennas as in Fig. 2 (d)), one contact out of many might also need to be selected. Henceforth, we embrace and model all this spacecraft restrictions under a maximum quantity of *simultaneous communication links* each node can implement at a given time.

In general, constraints require a selection process among conflicting contacts. To illustrate the latter, suppose that the SSN in Fig. 1 makes use of the architecture shown in Fig. 2 (b). Given that the nodes in this example account for two antennas but a single transmitting resource (i.e. a single communication link per satellite), a decision must be taken for N_2 and N_3 at k_3, k_4, and k_5 of the contact topology. Indeed, two possible outcomes for the first half orbit are illustrated in Fig. 3 (a) and (b). If the first one is chosen, the network will provide maximum overall (i.e. system-level) system contact time, while if the second one is selected a more fair and connected network will be obtained. Both solutions can be implemented with the specified SSN architecture and resources; however, they honor different selection criteria: overall system throughput or link assignment fairness.

As a result, only a given group of contacts contained in the contact topology list will be finally considered for implementation in the final SSN during the specified time interval. In particular, this resulting set is the *contact plan*. We refer to the process of deriving the latter from the contact topology by the name of *contact plan design* (CPD) procedure. In other words, the CPD takes a contact topology to finally deliver a contact plan that encodes all forthcoming network transmission opportunities that complies with resource restrictions and maximizes a given performance metric. In general, the CPD derives in a non-trivial combinatorial problem

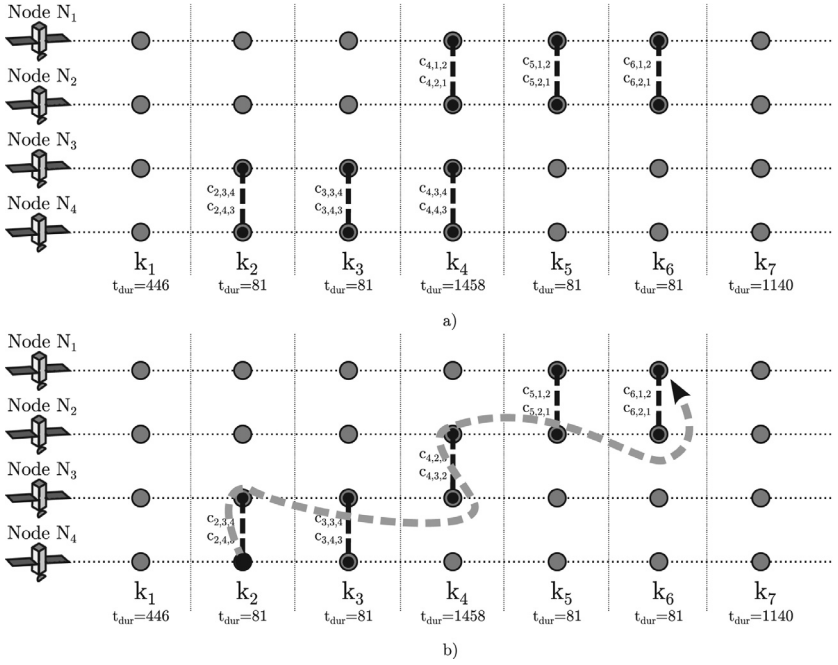

Fig. 3. Two possible contact plans for the example SSN: (a) Maximum throughput and (b) Link fairness.

with exponentially increasing complexity that must be solved before defining and distributing the final contact plan to the SSN.

Among existing CPD schemes, Fair Contact Plan (FCP) [25] is probably the simplest one as it only exploits the topology information to solve the design problem. FCP performs a fair assignment of single-hop links among nodes along the time interval while honoring resource constraints. In particular, starting from an empty contact topology, FCP iterates through states enabling as much contacts as possible prioritizing those with less occurrences on previous states. However, since the simplicity of FCP ignores the impact of each contact on system-level multi-hop routes, Route-Aware Contact Plan (RACP) [26] scheme generally delivers better connected contact plans. RACP achieves this by combining existing DTN routing algorithms with meta-heuristic exploration procedures to generate contact plans with low delivery-time routes. We suggest the interested reader to refer to [25,26] for additional details on these schemes. Most importantly, both FCP and RACP assumes an unknown traffic matrix leaving room for further tuning the resulting contact plan when the data generation can be predictable as in many SSNs systems.

In this work, we enhance the efficiency of FCP and RACP schemes by also considering the predictability of forthcoming traffic. Indeed, planning ahead considering basic storage and transmission capacity combined with resources constrains to determine the optimal flow of traffic can certainly result challenging for the average network operator. Therefore, in Section 3 we propose a MILP model capable of automatically determine efficient contact plans to support connectivity among resource constrained DTN nodes by exploiting the traffic predictability of SSNs.

3. Traffic-aware contact plan design

As previously stated, the problem of CPD lies on selecting among those contacts that satisfy the communication opportunities represented in the contact topology, fulfill resource constraints discussed in Section 2.2, and optimize the topology by a given criterion. We also argued that in the particular case of Earth Observation SSN missions, network traffic is generally predictable as it is generated by an operator demand (i.e. instrument or payload acquisition) while the system topology can be predicted by combining orbital dynamics and communication models. Under these assumptions, we propose traffic-aware contact plan (TACP): a MILP formulation of the CPD process for these scenarios. In general, a MILP formulation stands for a restricted optimization problem where some of its variables are restricted over the integers such as those required for combinatorial selections. Indeed, the output of TACP is an optimal routing and forwarding assignment that minimizes overall delivery delay for the specified traffic while providing an optimal selection of communication resources. As we further explain in this section, an efficient contact plan can be directly derived and implemented out of this optimal flow assignation by enabling those contacts expected to carry data.

3.1. TACP parameters and variables

Basically, the TACP formulation represents the topology as a function of time by using a finite state machine statement as illustrated in Fig. 1. Therefore, the MILP formulation assumes the time is discretized and encoded in $T = \{t_k\}$ and $I = \{i_k\}$ matrices as explained in Section 2.1. However, since the decision granularity of the model is based on the arcs stored on each state, interval fractionation might result convenient to increase TACP efficiency. In particular, fractionation implies that any k_i state can be deliberately divided into two new states k_{i_a} and k_{i_b} (implying $t_i = t_{i_a} + t_{i_b}$). For example, in the topology of Fig. 1, k_4 with a total duration of $i_4 = 1458$ s could be conveniently splitted in 3 states of $i_{4a} = 500$ s, $i_{4b} = 500$ s, and $i_{4c} = 458$ s as we later propose in Section 4. Although k_{i_a} and k_{i_b} still have the same associated graph than k_i, a CPD procedure can take independent decisions on each of these 3 arcs. In the resulting contact plan, the latter phenomena might be noticed as a contact shortening effect. In general, fractionation allows for a finer design granularity which might improve contact plan accuracy at the expense of computation complexity as we later discuss in Section 5.

In order to model the traffic flow in the network model, the evaluated contact topology needs to be expressed as a set of arc capacities $c_{k,\,i,\,j}$ between node i and j for each k state as illustrated in Fig. 1. In other words, there is a $c_{k,\,i,\,j}$ for each state k

representing the traffic volume node i can transfer to j between $[t_{k-1}, t_k]$. Therefore, every arc in the model has an associated data capacity which combined with the state duration can then be mapped to the link data-rate ($c_{k,i,j} = rate_{i,k} * (t_k - t_{k-1})$) normally used in ION [16] contact plan format. In particular, we assume $c_{k,i,j} = 0$ implies no transmission (i.e. contact) is feasible between i and j. As a result, the complete contact topology can be modeled by a $C_{k,i,j}$ matrix of size $K \times N \times N$ encompassing the existing contact opportunities for all N nodes and their corresponding capacities discretized in K states.

Since DTN implements a store-carry-and-forward scheme, the overall system capacity is not only related to link transfer (as expressed in C) but also to the storage capability of each intermediate node. Therefore, in addition to the contact capacity information, the MILP statement assumes each vertex i has an associated maximum buffer capacity of b_i. Consequently, the effective buffer usage for each i node at each k by a data sent from y to z is modeled in a set of $B^{y,z}_{k,i}$ variables. Noticeably, the summation of all $B^{y,z}_{k,i}$ for all y, z and k, should never exceed b_i. Therefore, in addition to link capacity matrix C, a storage matrix $B = \{b_i\}$ of size N is taken as input to properly characterize these basic restrictions discussed in Section 2.2. Due to their combinatorial nature, we will consider constraints in the formulation of TACP in Section 3.2.

The expected source flow demand is expressed as a traffic matrix D (where $D = \{d^{i,j}_k\}$) which is known in advance as previously discussed. In particular, such a traffic plan is formed by a set of $d^{i,j}_k$ traffic volumes representing data to be generated at the beginning of state k (at time t_{k-1}) at node i with j as final destination. It should be noticed that the MILP model as formulated allows for multiple data generation points throughout the topology time, even for the same source and destination tuple (i, j) in different states. When traffic generation is expected to happen within a given k, fractionation can be implemented to precisely model the creation time of the flow. Finally, the units of C, B and D should all represent traffic volume and are typically bits, bytes, or packets if their size is constant. Also, if nodes data-rates are equal, traffic volume can be directly mapped to time (channel access time) which can also be used as unit.

The resulting traffic flow is captured by means of $X^{y,z}_{k,i,j}$ variables representing the transmission with source y and destination z flowing through node i to j at state k. In general, the summation of these flows should never exceed the associated arc capacity $c_{k,i,j}$ or provoke a buffer (b_i) overflow in the receiving node i. Besides, it is worth clarifying that since we are modeling LEO SSNs, the stated model only accounts for disruptions, disregarding delays in the network. This means that flow $X^{y,z}_{k,i,j}$ is assumed to instantly propagate from node i to node j at the corresponding data rate $rate_{i,k} = c_{k,i,j}/i_k$. However, the model can easily be generalized to incorporate the delay phenomena typical of deep space systems by including a delay parameter in each contact as in [27].

Once the contact topology C, the buffer capacity B, and the traffic plan D are defined, the model should be capable of providing an optimal flow assignment to each of the $X^{y,z}_{k,i,j}$ variables. At this stage, the MILP model can be used as a centralized routing scheme as further discussed in Section 4.1. However, as previously detailed in Section 2.2, constraints need to be applied before calculating the final contact plan. In order to model this combinatorial resource constraints, we include another matrix $P = \{p_i\}$ whose p_i components encode the maximum quantity of communication links node i can simultaneously implement at a given time. Being able to choose more than one simultaneous link (i.e. two or more simultaneous antennas) is an exclusive property of this TACP statement since previous CPD procedures such as FCP [25] assumed the interface limitation was always $p_i = 1 \quad \forall i$. In order to model the combinatorial nature of the interface selection, we include a set of binary variables $Y_{k,i,j}$ which are meant to adopt a binary value of 1 if the link is used and 0 otherwise.

Table 2
TACP model parameters.

Input coefficients	
N	Nodes quantity
K	Topology states quantity
$T = \{t_k\}$	State k initialization time ($1 \le k \le K$)
$I = \{i_k\}$	State k interval duration ($i_k = t_k - t_{k-1} : 1 \le k \le K$)
$C = \{c_{k,i,j}\}$	Capacity of i to j contact at state k ($1 \le k \le K$ and $1 \le i, j \le N$)
$B = \{b_i\}$	Node i buffer capacity ($1 \le i \le N$)
$D = \{d^{i,j}_k\}$	Traffic from i to j originated at the beginning of k ($1 \le k \le K$ and $1 \le i, j \le N$)
$P = \{p_i\}$	Number of simultaneous links in node i ($1 \le i \le N$)
M	Big "M" coefficient for link equations
Output Variables	
$\{X^{y,z}_{k,i,j}\}$	Traffic from y to z at state k in i to j arc ($1 \le i, j, y, z \le N$)
$\{B^{y,z}_{k,i}\}$	Node i buffer occupancy at the end of k by traffic from y to z ($1 \le i, y, z \le N$)
$\{Y_{k,i,j}\}$	Interface selection from i to j at state k ($1 \le k \le K$ and $1 \le i, j \le N$)

As a result, TACP variables and parameters can be used to model a selection of the required link in each node that can optimize the delivery of the input traffic matrix D through a contact topology expressed in C with storages B while satisfying a link usage constraint modeled in P. In consequence, we further describe TACP formulation in Section 3.2 which is expected to deliver traffic flows in $X^{y,z}_{k,i,j}$, the buffer allocation required to store the information in $B^{y,z}_{k,i}$, and the optimal link selection in $Y_{k,i,j}$. The coefficients required as input for the MILP formulation and the resulting variables are summarized in Table 2.

3.2. TACP formulation

We define as the overall goal of the TACP model to use the minimal and earlier arcs to accommodate the flow detailed in D. In other words, we designed TACP objective to minimize the delivery time given the coefficients, variables and constraints previously defined in Section 3.1. Therefore, the problem can be formally expressed as an extension to the well-known multi-commodity flow problem [28] in Eqs. (1) to (9).

$$\text{minimize:} \quad \sum_{k=1}^{K}\sum_{i=1}^{N}\sum_{j=1}^{N}\sum_{y=1}^{N}\sum_{z=1}^{N} w(t_k) * X^{y,z}_{k,i,j} \tag{1}$$

Subject to:

$$\sum_{j=1}^{N} X^{y,z}_{k,j,i} - \sum_{j=1}^{N} X^{y,z}_{k,i,j} = B^{y,z}_{k,i} - (B^{y,z}_{k-1,i} + d^{i,z}_k) \quad \forall k, i, y, z \tag{2}$$

$$B^{y,z}_{k,i} <= b_i \quad \forall k, i, y, z \tag{3}$$

$$B^{y,z}_{0,i} = 0 \quad \forall i, y, z \tag{4}$$

$$\sum_{y=1}^{N}\sum_{z=1}^{N} X^{y,z}_{k,i,j} <= c_{k,i,j} \quad \forall k, i, j \tag{5}$$

$$\sum_{k=1}^{K}\sum_{j=1}^{N} X^{y,z}_{k,i,j} = \sum_{k=1}^{K} d^{i,j}_k \quad \forall i = y, z \tag{6}$$

$$\sum_{k=1}^{K}\sum_{i=1}^{N} X^{y,z}_{k,i,j} = \sum_{k=1}^{K} d^{i,j}_k \quad \forall y, j = z \tag{7}$$

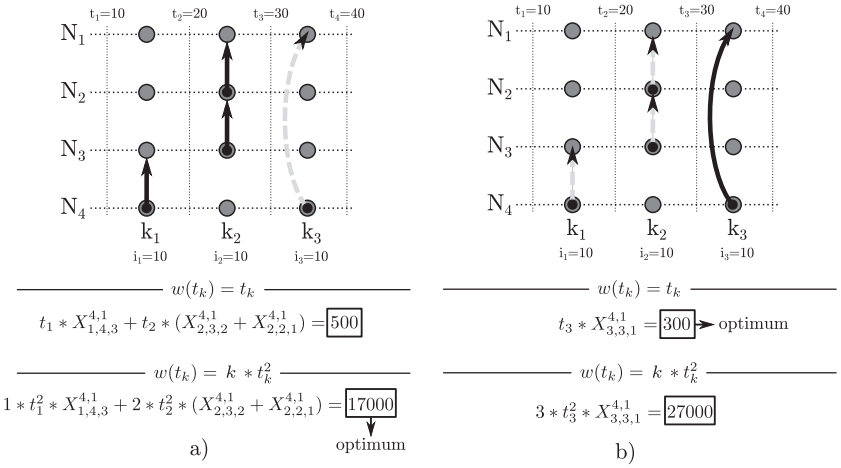

Fig. 4. TACP $w(t_k)$ coefficient in objective function.

$$\sum_{j=1}^{N} Y_{k,i,j} <= p_i \quad \forall i, k \tag{8}$$

$$\sum_{j=1}^{N}\sum_{y=1}^{N}\sum_{z=1}^{N} X_{k,i,j}^{y,z} <= M * Y_{k,i,j} \quad \forall i, k \tag{9}$$

The objective function (1) aims at minimizing the sum of the products of data units ($X_{k,i,j}^{y,z}$) with the time associated to the k state (t_k) modified by a weighting function $w(t_k)$. The higher the weighting, the more importance on the usage of earlier delivery paths (no matter how many arcs); and the lower $w(t_k)$, the less utilization of arcs throughout the topology. For example, consider the simple scenario illustrated in Fig. 4 where a single flow of $d_1^{4,1} = 10$ is expected to be delivered from N_4 to N_1 with two feasible paths: a) and b). If $w(t_k)$ coefficient is used with $w(t_k) = t_k$, the case b) minimizes the objective function to 300; however, although an efficient solution in terms of arc quantity, it does not provide the earliest delivery time possible. If delivery time is to be strictly optimized, several arcs in k_1 and k_2 ought to be elected instead of a single one in k_3; to achieve this effect, $w(t_k)$ coefficients might need to be further raised. For this example, we find that a $w(t_k) = k * t_k^2$ is enough to guarantee an earliest delivery time, being 17,000 and 27,000 the result of the objective function for Fig. 4 (a) and (b) respectively. It is worth emphasizing that t_k^2 is a coefficient and not a variable operation; therefore, the model remains linear. Also, as noticed, the value of the $w(t_k)$ coefficient might increase drastically and must be properly bounded in order to avoid overflows in existing MILP solver implementations. However, and since we will focus our analysis on networks with unique paths to the traffic destination, we leave the determination of a general formulation of $w(t_k)$ as further work. To summarize, the TACP MILP model as stated has a mixed yet customizable objective of optimizing the delivery time of the maximum traffic volume while minimizing the contact usage.

Among the constraints, Eq. (2) maps the flow imbalance in each node i to its buffer variation for all states and each (y, z) flow. Moreover, $d_k^{i,z}$ is included in the imbalance modeling the spontaneous generation of traffic in i with destination z. Therefore, $d_k^{i,z}$ is either transmitted (increasing $X_{k,i,j}^{y,z}$) or stored in the local buffer (increasing $B_{k,i}^{y,z}$). Eqs. (3) and (4) impose an upper bound b_i and an initial empty condition $B_{0,i}^{y,z} = 0$ for each node i and y, z flow respectively. For upcoming states $k > 0$, buffer occupation will be able to increase both by the generation of $d_k^{i,z} > 0$ or the reception of flows from other nodes $X_{k,j,i}^{y,z}$ and decrease by the transmission of them. The maximum capacity for each arc is enforced in (5). In particular, if all nodes transmit with the same data-rate, all arcs spanning a given contact will have the same $c_{k,i,j}$ value. Next, all source (node i is the traffic source y) and sink (node j is the traffic destination z) outflow and inflow imbalance is generated by (6) and (7) respectively. In other words, these equations force the transmitting node to effectively send all generated data and the receiver node to sink it. Also, Eq. (2) avoids to send a given $d_k^{i,z}$ before the specific k were it is supposed to be generated. As a result, Eqs. (2) to (7) model the contact topology and buffer capacity limitations and enforce traffic transmission and reception.

Furthermore, Eqs. (8) and (9) models constraints by limiting the maximum quantity of simultaneous links to use in a given node i. In particular, Eq. (8) verifies that the summation of the binary variables $Y_{k,i,j}$ meets the p_i bound. On the other hand, Eq. (9) binds the link selection with the activation of the $X_{k,j,i}^{y,z}$ commodities that flows through it. Therefore, if a link is not elected, the corresponding forward and return traffic in the associated arc should be 0. To this end, we use an existing LP modeling strategy known as "big-M" [29] as we describe next. When a given link is enabled, a sufficiently big coefficient M multiplies the binary variable $Y_{k,i,j}$ so as to permit the left part of the Eq. (9) to rise without limitations. Since this part of the equation includes the flows associated to that specific contact, this means they are allowed to course data. On the other hand, when a link is disabled, $M * Y_{k,i,j} = 0$, forcing all $X_{k,j,i}^{y,z}$ flows on the other side of the equation to be 0, implying no traffic can be sent on the disabled contact. To achieve this behavior, the M coefficient must be bigger than the summation of all the possible traffic flowing through that link (i.e. $M > c_{k,i,j}$). Even though Eq. (9) allows the model to include a valid mean to select a given link quantity, the "big-M" approach is known to provoke numerical instability problems specially for $M >> \sum X_{k,j,i}^{y,z}$ [29]. Therefore, M should be carefully chosen to satisfy the requirement of the equation while remaining as small as possible.

Besides, as stated in Eqs. (1) to (9), TACP supports link limitations $p_i > 1$ implying that a given node i can have simultaneous contacts becoming an intermediate node between a seamless data flow between two or more neighbors at a given k state. For instance, if two neighbors A and C have overlapping contacts with an intermediate node B, its buffer $B_{k,B}^{y,z}$ will not be affected by this particular transaction as the output flow $X_{k,B,C}^{y,z}$ will compensate input flow $X_{k,A,B}^{y,z}$. Therefore, TACP is designed to support CPD with contact overlapping in a single node when spacecraft resources permit.

At this stage, TACP model is able to efficiently combine the information of the predictable topology and the planned traffic of

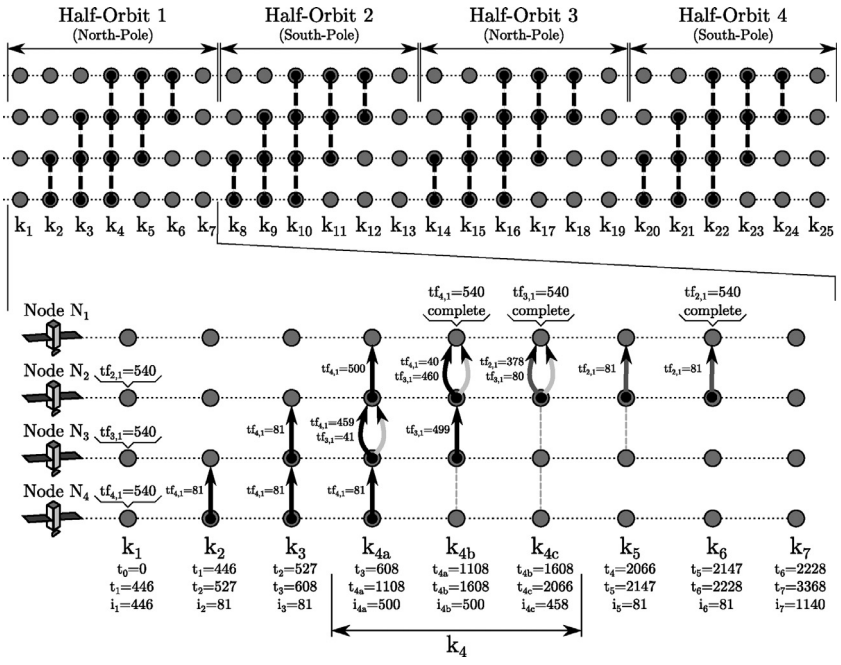

Fig. 5. Resulting traffic flow in unconstrained contact topology for $\rho = 1$.

the SSN to provide an efficient flow assignation considering the CPD constraints. Indeed, this assignment expressed in flow variables can be directly mapped to corresponding contacts of the final contact plan. In particular, the summation $\sum X^{y,z}_{k,i,j} \quad \forall y, z$ corresponds with the total allocated capacity of the arc between i and j, within the t_k and t_{k+1} time frame. Indeed, a summation of 0 implies that the k, i, j arc is either nonexistent in the contact topology, or that it is not coursing traffic after applying TACP. Finally, subsequent arcs between t_k and t_{k+n} can be concatenated into a single contact to be finally added to the resulting contact plan suitable of being provisioned to the orbiting SSN. In the following section we analyze TACP performance in a particular case study to later discuss computing complexity and applicability considerations in operative SSNs in Section 5.

4. Performance analysis

In this Section we use the example SSN presented in Section 3 to evaluate and compare TACP performance with existing CPD procedures such as FCP [25] and RACP [26] overviewed in Section 2.2. We also include the plain contact topology (henceforth referred to as CT) in the comparison to illustrate how the resource restriction impacts in the final traffic flow performance.

4.1. Case study overview

A total of 25 states is used to represent the SSN topology within the time interval which includes 4 over the pole communication opportunities. However, as previously explained in Section 3, in order to allow finer granularity and accuracy in the CPD, the topology states with arcs longer than 500s ($i_k > 500$) are further partitioned into sub-states. In this particular topology, the fractionation effect is illustrated in the lower part of Fig. 5 where state k_4 is deliberately subdivided in k_{4a}, k_{4b}, and k_{4c} of $i_{4a} = 500s$, $i_{4b} = 500s$, and $i_{4c} = 458s$. Indeed, k_{10}, k_{16} k_{22} has the same arc duration than k_4 and are therefore also fractionated. We will further discuss and generalize the fractionation criterion in Section 5.

In order to compare the stated CPD procedures, we need to define a traffic forwarding scheme to route data-flows in the resulting contact plan. To this end, we reuse the routing capability of the multi-commodity flow formulation previously explained in Section 3. In particular, an optimal flow assignation can be obtained by feeding the obtained contact plan to the MILP model considering only the restrictions of Eqs. (2) to (7) while disregarding Eqs. (8) and (9). The interested read can refer to [27] for further details on this MILP-based routing scheme. In addition, the resulting routing scheme assumes no propagation delay properly mimicking LEO SSNs. As we further discuss in Section 5, this routing decisions are optimal and based on a global view of the network which might differ from a distributed scenario where forwarding decisions are based on each node's local view of the topology such as CGR [14].

In order to mimic typical Earth observation instrumentation acquisitions in the Equator area, we configure the SSN to equitably generate downlink traffic in all N_2, N_3 and N_4 nodes at the beginning of the topology (k_1). Next, the traffic can flow towards N_1 who is expected to later deliver the data by means of a space-to-earth high speed downlink transponder. On board communication systems are constrained to up to one inter-satellite link per node configured with a $1Mb/s$ full-duplex throughput within a maximum range of 700 Km. For sake of simplicity, transmitted packet sizes are set to $1Mbit$ or $125KByte$ which at $1Mb/s$ occupies the channel for $1s$. It is worth noting that since the topology is based on the combination of orbital dynamic and communications models between two nodes, the contacts are considered feasible when enough link margin guarantees an error-free transmission (in this example a range of 700 Km). Therefore, the overhead imposed by retransmission schemes or any collision-based shared medium access technique can be disregarded in the general case. Nonetheless, in Section 5.1 we consider adding margins that might accommodate these marginal scenarios at the CPD stage.

In this scenario, we study the saturation flow for the CT contact plan where the optimal flow assignation allows the successful delivery of the three source flows of 540 packets from N_2, N_3 and N_4 to N_1 as shown in Fig. 5. In addition, buffer capacities b_i are configured to accommodate this traffic without overruns for all i nodes, leaving storage analysis as further work. Within Fig. 5, each traffic flow from node N_A to node N_B is measured in packets

Table 3
Case study TACP model parameters.

Input coefficients	
N	4 nodes
K	25 states
$T = \{t_k\}$	{0, 446, 527, 608, 1108, 1608, 2066, 2147, 2228, ...} s
$I = \{i_k\}$	{446, 81, 81, 500, 500, 458, 81, 81, 1140, ...} s
$C = \{c_{k,i,j}\}$	$c_{k,i,j} = i_k \times 1$ Mb/s $\quad \forall k, i, j$
$B = \{b_i\}$	$b_i = 3 \times 540$ Mbit $\quad \forall i$
$D = \{d_k^{i,j}\}$	$d_0^{2,1} = d_0^{3,1} = d_0^{3,1} = 54...540$ Mbit
$P = \{p_i\}$	$p_i = 1 \quad \forall i$
M	5000

(equivalent to seconds in this particular case) and measured by parameter $tf_{A,B}$. It should be noticed that no further data can flow to N_1 in this orbit as the contact spanning k_4 to k_6 has a duration of 1620 s which is the limit to accommodate $540 \times 3 = 1620$ source packets of 1 s duration each. Therefore, although other contacts such as N_4 to N_3 (k_{4b} and k_{4c}) and N_3 to N_2 (k_{4c} and k_5) remains underutilized, this flow configuration represents the network saturation for a single orbit of the proposed SSN and is selected as the maximum evaluation traffic. However, such a performance is only achievable when link restrictions are ignored since N_2 and N_3 are simultaneously transmitting and receiving data at k_3, k_{4a}, and k_{4b}. If the interface restriction is applied, the final delivery time must be postponed until further contacts become available in the upcoming orbits. Therefore, in the present analysis we vary the traffic load from $\rho = 1$ (540*Mbit*, 67.5*MByte* or 540 packets per node) down to $\rho = 0.1$ (54*Mbit*, 6.75*MByte* or 54 packets per node). All TACP model parameters for this particular case study are summarized in Table 3.

In order to compare the different strategies, it is necessary to measure and understand how efficiently the delivery of the traffic is, which is determined by the CPD procedure efficiency. To measure this efficiency, we define and monitor (a) the payload data *delivery time* and (b) the overall *system contact time*. The former metric stands for the time within the time interval at which all traffic generated in the SSN system is delivered to the final destination. In our particular case study, it is the time when all $d_0^{2,1}$, $d_0^{3,1}$, and $d_0^{3,1}$ flows reaches N_1 (i.e., all packets delivered). On the other hand, the system contact time measures the overall contact utilization of all nodes during this time frame. Specifically, since the system contact time is the summation of the time the transponders are enabled in the SSN, it can be used as a direct measure of resource usage in terms of power consumption within the time interval. Indeed, both metrics are expressed in time units and the lower their value, the more efficient the CPD procedure. As further discussed in Section 5, the final utilization of contacts and resources in a SSN will also depend on the routing and forwarding scheme implemented on the nodes which is assumed optimal in our analysis.

Finally, we configure RACP meta-heristic iterations to 10000 with a maximum temperature of 10000 and an all-to-all multi-hop delay improvement criteria. These values are provided as configuration reference for the reader interested in replicating this comparison: please refer to [26] for a complete description of RACP parameters. Also, we set $w(t_k) = t_k$ in the TACP model but it has no relevance in the resulting contact plan since there is only a single feasible path to N_1 (N_4 to N_3 to N_2 to N_1). We leave the analysis of different $w(t_k)$ coefficients for further work encompassing multi-path scenarios. In addition, the TACP model summarized in Table 3 has been implemented and solved using GLPK v4.56 [30], a free Linux-based MILP solver which is able to provide optimal solutions in less than a minute when executed on a Intel i-5 processor with 4 GB of RAM. Finally, the results of this configurations are summarized and reviewed in Section 4.2.

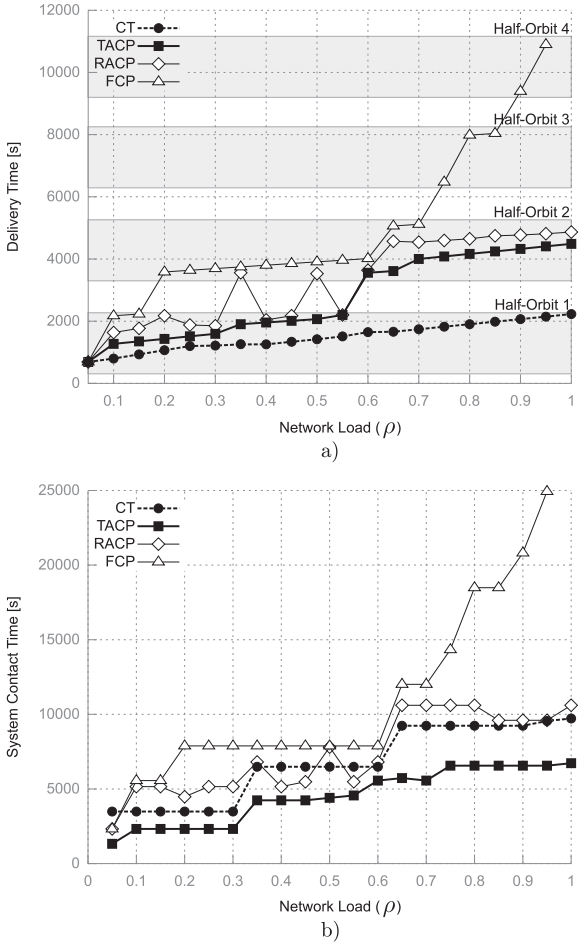

Fig. 6. Case Study (a) delivery time and (b) system contact time for varying ρ.

4.2. Case study results

The *delivery time*, and *system contact time* metrics obtained with a varying network load ($0 \leq \rho \leq 1$) for the unconstrained contact topology (CT) and each CPD scheme (TACP, RACP, and FCP) are plotted in Fig. 6(a) and (b) respectively. In particular, the delivery time curve in Fig. 6 (a) also highlights the 4 contact opportunity windows over the pole of the SSN case study. Therefore, all deliveries to N_1 fall within the duration of these connectivity intervals. Indeed, if the delivery could not be completed in a given over-the-pole fly-over, it continues in the next one and so forth until the traffic to N_1 is completely evacuated.

The delivery time of the CT in Fig. 6 (a) increases up to 2228*s* for $\rho = 1$, which is precisely the time when state k_6 and the first orbital period ends (Fig. 5). On the system contact time, the CT plan evidences an increase of this metric each time the traffic flow requires a new state for forwarding the data. It is worth clarifying that this metric only considers all enabled arcs until the delivery of traffic in the SSN is complete. For example, for $\rho = 0.3$ the delivery is completed at 1094*s* which is within k_4, while for $\rho = 0.35$ it is 1175*s* which correspond to state k_5. In this evolution of ρ, a new arc is required to accommodate the flow and therefore, since the CT has not only N_2 to N_1 link enabled but all others arcs (N_4 to N_3 and N_3 to N_2), the overall system contact time increases drastically. In general, routing data using the contact topology always provide the best delivery time as it accounts for all the network contacts and resources. However, the latter implies that several arcs might remain underutilized increasing the system contact time.

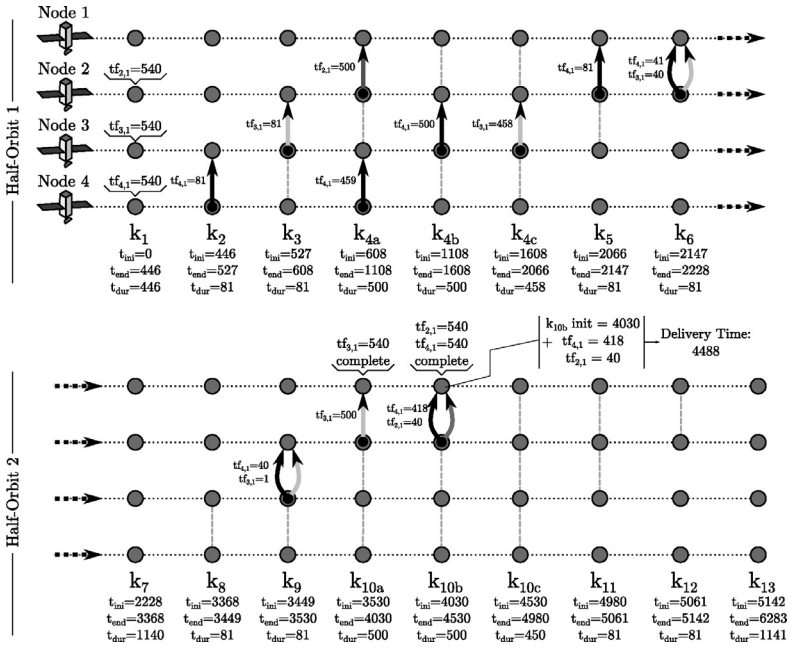

Fig. 7. TACP contact plan for $\rho = 1$.

When considering TACP model, the overall system contact time is optimized as every enabled arc in the final contact plan is used by the flowing traffic (retransmissions due to channel errors are disregarded). Indeed, all remaining arcs are disabled and none of them remains underutilized. This allows TACP to be the most effective scheme in terms of system resource usage; however, as discussed in Section 5, it might require the inclusion of error margins in case of traffic planning discrepancies. Regarding delivery time (Fig. 6 (a)), TACP is not able to provide the CT performance due to resource restrictions. This is because CT exploits simultaneous interface usage as illustrated in Fig. 5, while TACP, RACP and FCP are configured not to use more than one arc in any node within a given state. Among these resource-aware CPD mechanisms, TACP provides the best delivery time for all ρ. In particular, the optimal CPD for $\rho = 1$ is illustrated in Fig. 7 for which the TACP contact plan provides a delivery time of 4488s in state k_{10b} (2nd half-orbit period). It is interesting to note in this figure that no node uses more than one arc at all times, and that given this condition, the MILP formulation guarantees this is the optimal solution in terms of delivery time.

TACP is closely followed by RACP in terms of CPD performance. Since RACP implements heuristic algorithms to explore the feasible contact topology solution space while evaluating multi-path metrics, it can probabilistically find very suitable contact plans. In fact, RACP performs better than expected by providing contact plans with delivery time as low as TACP for certain ρ but without the need of exploiting traffic volume predictability. However, since RACP does not incorporate information on the network traffic, it enables arcs with the aim of favoring an all-to-all multi-path flow. Consequently, the RACP contact plan evidences several underutilized arcs which makes the system contact time metric considerably higher than TACP.

Finally, we analyze FCP, the simplest CPD mechanism in terms of network information but probably the most efficient in terms of computation complexity. Because of the usage of the Blossom algorithm [31], FCP procedure certainly outperforms the processing time RACP and TACP requires to design a contact plan. However, since FCP only evaluates single-hop contacts in order to maximize a fairness metric [25], the resulting contact plan provides no particular benefit to the specificity of the traffic flow. As a consequence, FCP-designed contact plan requires significantly longer time to deliver the traffic completing its delivery in the 4th half-orbit of the example SSN topology. Such a late delivery has a severe impact on the amount of system resources required until the flow reaches its final destination (N_1).

To summarize the case study, TACP outperformed the most efficient CPD scheme (RACP) by 42% in terms of system resource usage while also improved the delivery time by a 10% for $\rho = 1$. This performance improvement might become more significant for larger topologies where a bad contact selection can derive in severe system-wide traffic delays; however, we leave the analysis of more complex escenarios as further work. Last but not least, this improvement comes at a cost in terms of computation complexity, and lack of flexibility in TACP respect to previous CPD procedures. In Section 5 we review these limitations and also discuss general recommendations for the implementation of TACP in operative SSN systems.

5. Discussion

5.1. TACP considerations and limitations

TACP complexity: The proposed TACP model is the most complex CPD scheme to the best of our knowledge at the time of writing. It models all relevant variables of the CPD process ranging from contacts, capacity, storage, resource constraints, traffic, routing, among others to deliver optimal contact plans for small-sized SSN systems as shown throughout this work. However, this comes at a complexity cost where matrices of $N \times N \times K$ elements impose severe scaling limitations specially when considering networks with several orbiting nodes, various traffic sources, long time intervals, or fine state fractionation. Therefore, the authors are currently working and experimenting on algorithmic and sub-optimal heuristic alternatives to solve the CPD process with traffic consideration for these complex scenarios. To this end, the presented TACP model is playing an important role as a CPD performance bound to evaluate these emerging developments.

TACP inflexibility: As shown in Section 4, TACP scheme provides the best contact plans in term of delivery delay and system

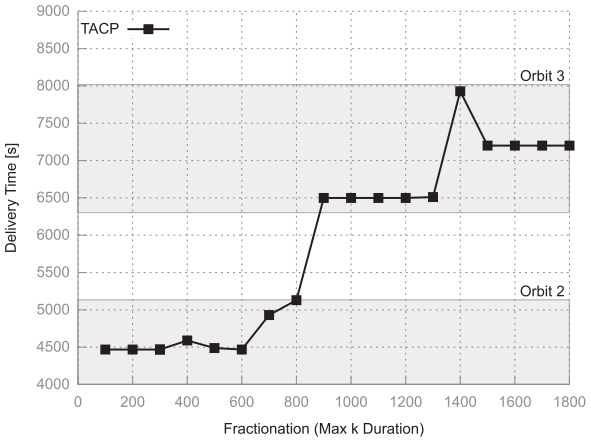

Fig. 8. TACP Contact Plan Delivery time for $\rho = 1$ and varying fractionation.

contact time. However, this is achieved by exploiting both topology and traffic information which are assumed to be complete and accurate enough. If further unplanned traffic is to be generated, or retransmission schemes make unpredictable usage of the capacity, the consequences could be severe as the exceeding information in the network might utilize the resources originally reserved to allocate the predicted traffic. This effect is less probable when using traffic-agnostic techniques such as RACP and FCP as they generally enable several arcs throughout the time interval allowing for a reallocation of the traffic. As a way to mitigate this phenomenon we discuss two possible approaches:

1. Including traffic safe-guard margins: This can be achieved by reserving certain data volume in $d_k^{i,j}$ parameters by a factor that represents the expected overhead. Indeed, these margins would depend on each particular scenario and their estimation should be made carefully and kept at minimum; otherwise, TACP performance degradation might result comparable with RACP scheme. Actually, when the unpredictable traffic becomes comparable to the predictable one, further studies would be required to determine the better scheme between RACP and TACP. Since the latter is considered a mixed traffic scenario, we leave their analysis as future work.
2. Enabling idle contacts: As previously stated, TACP only enables the contacts required to course the scheduled traffic in D. For instance, Fig. 7 shows that several communication resources remain unused in states k_{10a}, k_{10b}, k_{10c} and so forth. As a result, the operator might decide to enable them as a backup mechanism for unexpected traffic. The mechanism to execute this secondary decision can be based on RACP, but further exploration of these hybrid approaches towards CPD is required and therefore, also left as further work.

TACP topology granularity: As previously stated and described in Section 3, the fractionation of a state k_a in shorter states k_{a1} and k_{a2} allows the CPD schemes to account for a finer granularity in their arc assignments which in turn enable more efficient contact plans. Fig. 8 illustrates the delivery time metric for TACP with $\rho = 1$ for a varying fractionation parameter. In the example of Section 4, we found that a fractionation of states larger than 500 provided a metric of 4488s allowing for a balanced parameter in terms of CPD optimality and model complexity. As expected, for longer states, the model loses accuracy deriving in lower quality contact plans. However, as the fractionation granularity gets finer, the model becomes more complex requiring an exponentially increasing computing power to solve it in reasonable time. Furthermore, a highly partitioned plan might evidence performance issues due to the increase of communications changes and interruptions making the system more sensitive to synchronism offset between SSN nodes. Therefore, the fractionation parameter is certainly dependent on the specific TACP scenario which must seek for a balance between model complexity and CPD accuracy.

5.2. General CPD considerations

Contact plan computation element: It should be noticed that even though the proposed SSN scenario is composed of a rather limited number of nodes (4) and a short time interval (3 h 30 min), the analysis required to understand and validate a given contact can be considerable, especially for highly fractionated topologies. Furthermore, and in general, several CPD methodologies might be combined to design a contact plan for a specific SSN. For instance, an operator might have a combination of predictable traffic and sporadic unknown telemetry for which TACP can be used as a primary resource allocator while using RACP as a secondary design scheme for the remaining of the topology resources. Indeed, the overall complexity of these procedures might result challenging for the average network operator. Therefore, we envision a contact plan computation element (CPCE) which can assist or even automate the design of CPs for future spaceborne SSNs. A CPCE shall be capable of determining suitable CPs to support connectivity among nodes and data transfers through the network and would typically be part of the MOC center. Specifically, a CPCE would have to be executed in a periodic basis in order to later distribute and update the designed contact plan to the SSN as discussed below.

Contact plan distribution: Once the CPD is completed, the problem of contact plan distribution needs to be solved in order to allow nodes to finally use it as topological information. Even though dedicated effort to the proper and efficient design of contact plans for SSNs, there is further work necessary regarding the means by which the designed contact plans can safely reach each of the orbiting nodes through the same network. It is worth clarifying that these CPs are a key resource for each satellite to take routing and forwarding decisions by using contact-graph based schemes such as CGR [32]. There are previous works on the development of protocols to this end such as Contact Plan Update Protocol (CPUP) [33] that allows to distribute CPs in-band via Bundle Protocol. Nevertheless, the specific procedure of network bring-up during the commissioning phase remains an implementation and mission-specific issue.

Contact plan routing: A last but not least important consideration to be discussed is the routing scheme the final orbiting nodes will use to route and forward data. As previously stated in Section 4.1, the traffic model used in the case study to evaluate the designed contact plans is a MILP formulation of the multi-commodity flow problem that provides optimal flow assignations. However, SSN nodes routers are generally based on sub-optimal distributed routing schemes such as CGR [32]. Since this type of routing schemes uses only the topology information imprinted in the contact plan (e.g., disregarding remote traffic schedules), the resulting traffic flows might differ from those calculated by the MILP models generating unwanted congestion problems [34]. Although several CGR improvements such as [34–37] has been proposed to mitigate congestion, their behavior still can differ from the optimal assignation assumed in MILP-based CPD such as TACP. Indeed, since any discrepancies might result in traffic flowing through different contacts than those considered on the planning stage, they must be assessed to avoid dissipating the optimization obtained in the CPD procedure. At the time of writing, authors are supporting this assessment with detailed system simulations that validates that the sub-optimal algorithm behaves properly on the resulting contact plan.

6. Conclusion

Since outer space missions have to perform in a hardly accessible and extremely harsh environment, they become particularly expensive and limited in terms of lifetime. Therefore, we sought the improvement of the data delivery time and resource usage of Earth observation missions based on distributed sensor networks. Since Internet-based protocols fail to perform in this context, DTN store-carry-and-forward approach provides an appealing alternative. Among the challenges to effectively implement DTNs in space, we provided a thorough analysis of the problem and challenges of the contact plan design.

As a result, we investigated specific modeling techniques and contributed with TACP as a general, unique and novel CPD mechanism. Particularly, TACP takes advantage of the forthcoming traffic and topology information typically available in Earth observation SSNs to optimize the design of their contact plans. Finally, by designing the contact plan for an appealing LEO SSN topology, we demonstrated TACP outperforms existing CPD schemes by up to 42% in terms of system resource usage and up to 10% of delivery time.

Nonetheless, we detected that TACP complexity requires alternative computational strategies in order to deliver efficient contact plans for large-sized SSN systems. As a result, we leave as further work the research and assessment of algorithmic and sub-optimal heuristic techniques to execute the CPD process in these complex scenarios.

References

[1] H. Rashvand, A. Abedi, J. Alcaraz-Calero, P. Mitchell, S. Mukhopadhyay, Wireless sensor systems for space and extreme environments: a review, Sensors J. IEEE 14 (11) (2014) 3955–3970, doi:10.1109/JSEN.2014.2357030.

[2] J. Chu, J. Guo, E. Gill, Fractionated space infrastructure for long-term earth observation missions, in: Aerospace Conference, 2013 IEEE, 2013, pp. 1–9, doi:10.1109/AERO.2013.6496854.

[3] W. Larson, J. Wertz, Space Mission Analysis and Design, 8, 3 edition, Microcosm, Inc., Torrance, CA (US), 1999.

[4] R.C. Durst, G.J. Miller, E.J. Travis, Tcp extensions for space communications, Wireless Networks 3 (5) (1997) 389–403, doi:10.1023/A:1019190124953.

[5] A. Krishnamurthy, R. Preis, Satellite formation, a mobile sensor network in space, in: Parallel and Distributed Processing Symposium, 2005. Proceedings. 19th IEEE International, 2005, p. 7, doi:10.1109/IPDPS.2005.387.

[6] C. Caini, H. Cruickshank, S. Farrell, M. Marchese, Delay and disruption tolerant networking (dtn): an alternative solution for future satellite networking applications, 99, 2011, pp. 1980–1997, doi:10.1109/JPROC.2011.2158378.

[7] S. Burleigh, A. Hooke, L. Torgerson, K. Fall, V. Cerf, B. Durst, K. Scott, H. Weiss, Delay-tolerant networking: an approach to interplanetary internet, Commun. Magazine, IEEE 41 (6) (2003) 128–136, doi:10.1109/MCOM.2003.1204759.

[8] A. McMahon, S. Farrell, Delay and disruption tolerant networking, IEEE Internet Computing 13 (6) (2009) 82–87. http://doi.ieeecomputersociety.org/10.1109/MIC.2009.127.

[9] K. Fall, A delay-tolerant network architecture for challenged internets, in: Proceedings of the 2003 Conference on Applications, Technologies, Architectures, and Protocols for Computer Communications, in: SIGCOMM '03, ACM, New York, NY, USA, 2003, pp. 27–34, doi:10.1145/863955.863960.

[10] Internet Engineering Task Force (IETF), Delay tolerant networking working group (DTNWG), (https://datatracker.ietf.org/wg/dtnwg/charter/).

[11] Consultative Committee for Space Data Systems (CCSDS), Delay tolerant networking working group (SIS-DTN), (http://cwe.ccsds.org/sis/default.aspx#_SIS-DTN).

[12] V. Cerf, et al., RFC-4838: delay-tolerant networking architecture, Network Working Group, IETF, 2007.

[13] K. Scott, S. Burleigh, RFC-5050: bundle protocol specification, Network Working Group, IETF, 2007.

[14] G. Araniti, N. Bezirgiannidis, E. Birrane, I. Bisio, S. Burleigh, C. Caini, M. Feldmann, M. Marchese, J. Segui, K. Suzuki, Contact graph routing in dtn space networks: overview, enhancements and performance, Commun. Magazine, IEEE 53 (3) (2015) 38–46, doi:10.1109/MCOM.2015.7060480.

[15] J. Wyatt, S. Burleigh, R. Jones, L. Torgerson, S. Wissler, Disruption tolerant networking flight validation experiment on nasa's epoxi mission, in: Proceedings of the 2009 First International Conference on Advances in Satellite and Space Communications, in: SPACOMM '09, IEEE Computer Society, Washington, DC, USA, 2009, pp. 187–196, doi:10.1109/.38.

[16] S. Burleigh, Interplanetary overlay network: an implementation of the dtn bundle protocol, in: Consumer Communications and Networking Conference, 2007. CCNC 2007. 4th IEEE, 2007, pp. 222–226, doi:10.1109/CCNC.2007.51.

[17] W. Ivancic, W. Eddy, D. Stewart, L. Wood, P. Holliday, C. Jackson, J. Northam, Experience with delay-tolerant networking from orbit (2008) 173–178, doi:10.1109/ASMS.2008.37.

[18] S. Burleigh, V.G. Cerf, J. Crowcroft, V. Tsaoussidis, Space for internet and internet for space, Ad Hoc Netw. 23 (2014) 80–86, doi:10.1016/j.adhoc.2014.06.005.

[19] C. Caini, R. Firrincieli, Application of contact graph routing to leo satellite dtn communications, in: Communications (ICC), 2012 IEEE International Conference on, 2012, pp. 3301–3305, doi:10.1109/ICC.2012.6363686.

[20] D. Lary, An objectively optimized earth observing system, in: Aerospace Conference, 2007 IEEE, 2007, pp. 1–3, doi:10.1109/AERO.2007.353089.

[21] D.A. Vallado, Fundamentals of Astrodynamics and Applications - 4th Edition, Microcosm, Hawthorne, CA, 2007.

[22] J. Fraire, J. Finochietto, Design challenges in contact plans for disruption-tolerant satellite networks, Commun. Magazine, IEEE 53 (5) (2015) 163–169, doi:10.1109/MCOM.2015.7105656.

[23] H. Mendoza, G. Corral-Briones, Interferencia en sistemas distribuidos de satélites de orbita media y baja, in: XV Reunión de Trabajo Procesamiento de la Información y Control (RPIC), San Carlos de Bariloche, Argentina, 2013, pp. 1110–1115.

[24] P. Muri, J. McNair, A survey of communication sub-systems for intersatellite linked systems and cubesat missions, J. Commun. 7 (4) (2012) 290.

[25] J. Fraire, P. Madoery, J. Finochietto, On the design and analysis of fair contact plans in predictable delay-tolerant networks, Sensors J. IEEE 14 (11) (2014) 3874–3882, doi:10.1109/JSEN.2014.2348917.

[26] J. Fraire, J. Finochietto, Routing-aware fair contact plan design for predictable delay tolerant networks, Elsevier Ad-Hoc Netw. 25, Part B (2015) 303–313, doi:10.1016/j.adhoc.2014.07.006.

[27] J. Alonso, K. Fall, A linear programming formulation of flows over time with piecewise constant capacity and transit times, Techical Report, Intel, 2003.IR-B-TR-03-007

[28] T.H. Cormen, C. Stein, R.L. Rivest, C.E. Leiserson, Introduction to Algorithms, 2nd edition, McGraw-Hill Higher Education, 2001.

[29] I. Griva, S. Nash, A. Sofer, Linear and Nonlinear Optimization: Second Edition, Society for Industrial and Applied Mathematics (SIAM, 3600 Market Street, Floor 6, Philadelphia, PA 19104), 2009.

[30] Makhorin, Andrew, GLPK (GNU linear programming kit), 2015, (https://www.gnu.org/software/glpk/). Department for Applied Informatics, Moscow Aviation Institute, Moscow, Russia.

[31] V. Kolmogorov, Blossom v: a new implementation of a minimum cost perfect matching algorithm, Math. Program. Comput. 1 (1) (2009) 43–67, doi:10.1007/s12532-009-0002-8.

[32] S. Burleigh, Contact graph routing, IETF-Draft, 2010.

[33] N. Bezirgiannidis, F. Tsapeli, S. Diamantopoulos, V. Tsaoussidis, Towards flexibility and accuracy in space dtn communications, in: Proceedings of the 8th ACM MobiCom Workshop on Challenged Networks, in: CHANTS '13, ACM, New York, NY, USA, 2013, pp. 43–48, doi:10.1145/2505494.2505499.

[34] J. Fraire, P. Madoery, J. Finochietto, E. Birrane, Congestion modeling and management techniques for predictable disruption tolerant networks, in: 40th IEEE Conference on Local Computer Networks (LCN 2015), IEEE, 2015.

[35] E. Birrane, Congestion modeling in graph-routed delay tolerant networks with predictive capacity consumption, in: Global Communications Conference (GLOBECOM), 2013 IEEE, 2013, pp. 3016–3022, doi:10.1109/GLOCOM.2013.6831534.

[36] H. Yan, Q. Zhang, Y. Sun, Local information-based congestion control scheme for space delay/disruption tolerant networks, Wireless Netw. 21 (6) (2015) 2087–2099, doi:10.1007/s11276-015-0911-6.

[37] N. Bezirgiannidis, C. Caini, D.D.P. Montenero, M. Ruggieri, V. Tsaoussidis, Contact graph routing enhancements for delay tolerant space communications, in: 2014 7th Advanced Satellite Multimedia Systems Conference and the 13th Signal Processing for Space Communications Workshop (ASMS/SPSC), 2014, pp. 17–23, doi:10.1109/ASMS-SPSC.2014.6934518.

Juan A. Fraire received the Telecommunications Engineering degree at the Instituto Universitario Aeronáutico and his PhD in the National University of Córdoba (UNC). His research focuses on DTN networking for space-oriented applications. He is the communications protocol architect for STI Company where he is developing DTN solutions for earth-observation LEO constellation projects defined in the Argentinian Space Agency (CONAE) National Space Plan.

Pablo G. Madoery received the Telecommunications Engineering degree from the Instituto Universitario Aeronáutico, Argentina, in 2012. He has worked at the Digital Communication Laboratory of the National University of Córdoba in the field of satellite communications and currently he is starting a PhD in Engineering Sciences focusing his interest in models, algorithms and protocols for delay and disruption tolerant networks.

Jorge M. Finochietto is Full Professor at Universidad Nacional de Córdoba, Argentina (UNC), and Senior Researcher at the National Research Council (CONICET) of Argentina. Dr. Finochietto has been involved in several national and international research projects in the fields of communication networks. He has co-authored over 50 papers published in international journals and presented in leading international conferences.